

# Photothermally Induced Optical Property Changes of Poly(*N*-isopropylacrylamide) Microgel-Based Etalons

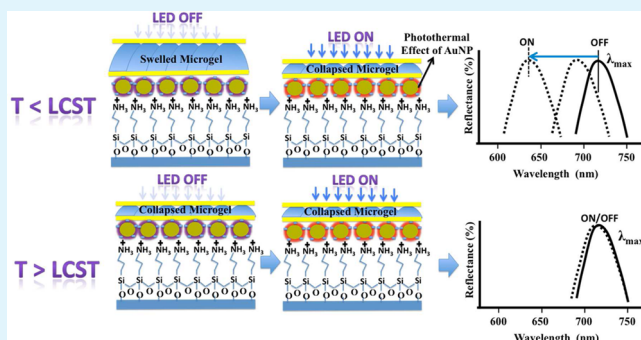
Molla R. Islam,<sup>†</sup> Jessica Irvine, and Michael J. Serpe<sup>\*</sup>

Department of Chemistry, University of Alberta, Edmonton, AB T6G 2G2, Canada

**S** Supporting Information

**ABSTRACT:** Poly(*N*-isopropylacrylamide) microgel-based optical devices were designed such that they can be stimulated to change their optical properties in response to light produced by a light-emitting diode (LED). The devices were fabricated by sandwiching the synthesized microgels between two Cr/Au layers all supported on a glass coverslip with gold nanoparticles (AuNPs) deposited. Here, we found that these devices can be stimulated to change their optical properties when exposed to green LED light, which excites the AuNPs and increases the local temperature, causing the thermoresponsive microgels to decrease in diameter, resulting in a change in the devices' optical properties. We also found that the sensitivity of the devices to light was more pronounced as the environmental temperature approached the lower critical solution temperature (LCST) for the microgels, although the sensitivity of the devices to light exposure dropped off dramatically as the environmental temperature was increased above the LCST. This was a direct result of the microgels already being in their collapsed state and therefore unable to decrease in diameter any further due to light exposure. Finally, we found that the sensitivity of the devices to light exposure increased with increasing number of AuNP layers in the devices. We anticipate that these devices could be used for drug delivery applications; by using light to stimulate microgel collapse, the microgel-based devices can be stimulated to release small molecules on demand.

**KEYWORDS:** poly(*N*-isopropylacrylamide) microgels, responsive polymers, light-responsive etalons, photothermal effect, gold nanoparticles, layer-by-layer assembly



## INTRODUCTION

Nanoparticles composed of various materials have emerged as excellent tools for achieving many new materials and material properties.<sup>1–5</sup> This is primarily due to their unique behavior that oftentimes varies significantly from their bulk counterparts, which can be used to achieve advanced materials. For example, unlike bulk Au, Au nanoparticles (AuNPs) are able to absorb visible light of specific wavelengths, as a result of surface plasmon resonance.<sup>6–8</sup> Heat is generated as a result of the absorption, which is able to increase the local temperature of systems. This photothermal effect has been exploited for various applications.<sup>4,9,10</sup>

“Responsive materials” or “smart materials” are also able to transform a stimulus into an observable physical or chemical change. Ideally, their response is reversible, and the materials revert back to their initial state once the stimulus is withdrawn. Polymer-based responsive materials, known as responsive polymers, are well-known and have been developed to respond to various stimuli, such as pH, temperature, analyte concentration, electric and magnetic fields, and biomolecules.<sup>11–15</sup> Poly(*N*-isopropylacrylamide) (pNIPAm) has become the most extensively studied responsive polymer over the decades.<sup>16–18</sup> pNIPAm is a well-known thermoresponsive polymer that undergoes a conformational change from an

extended coil to a compact globule in water when the temperature is raised  $>32$  °C, which is pNIPAm's lower critical solution temperature (LCST).<sup>19</sup> Above this temperature, pNIPAm transitions from a hydrophilic to a relatively hydrophobic state, where polymer–polymer interactions dominate. Like linear pNIPAm, cross-linked networks of pNIPAm (hydrogels) and colloidal stable hydrogel particles (microgels) can be synthesized, which also retain their thermoresponsive properties.<sup>16,20–22</sup> Hydrogels and microgel particles swell in water below the LCST of pNIPAm and shrink above the LCST reducing their volume and size. Additional functional/reactive/responsive groups can be incorporated into these pNIPAm-based materials at the time of synthesis to make them responsive to a number of different stimuli.<sup>23–27</sup> A variety of amines and/or carboxylic acid groups, for example, acrylic acid (AAc), methacrylic acid (MAAc), vinyl acetic acid, and *N*-(3-aminopropyl) methacrylamide hydrochloride (APMAH), can be introduced into the materials to achieve pNIPAm-based systems with novel chemistries and responsivities.<sup>13,17,28–31</sup>

**Received:** September 11, 2015

**Accepted:** October 20, 2015

**Published:** October 26, 2015

In previous studies, we showed that optical devices could be fabricated by sandwiching pNIPAm-based microgels between two Au layers supported on a glass substrate—the structure is shown schematically in Figure 1(a).<sup>32,33</sup> This device, referred to

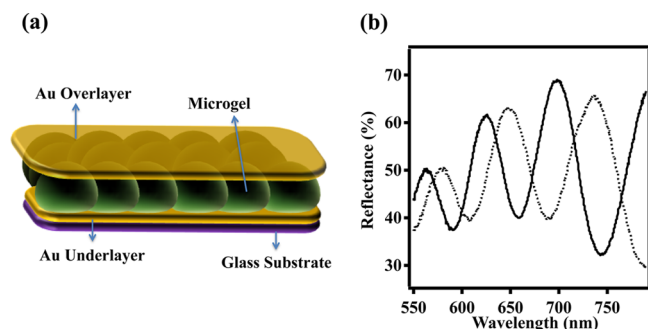


**Figure 1.** (a) Schematic of a microgel-based etalon. (b) A typical reflectance spectrum from a AuNP-loaded pNIPAm-co-AAc microgel-based etalon (solid line) before and (dotted line) after localized heating by exposure to a light-emitting diode emitting  $\sim 515$  nm light. The etalon is held at a temperature near the LCST for pNIPAm.

as an etalon, exhibits visible color and multiplex reflectance spectra as shown in Figure 1(b). The position of the peaks in the reflectance spectra depends on a number of factors according to eq 1

$$\lambda = (2nd \cos \theta) / m \quad (1)$$

where  $n$  is the refractive index of the microgel (dielectric) layer;  $d$  is the mirror–mirror distance;  $\theta$  is the angle of incident light relative to the device normal; and  $m$  (an integer) is the order of the spectral peak. We point out that while the device's optical properties depend on the parameters in eq 1 the mirror–mirror distance is primarily responsible for the tunable optical properties of our devices (at a single observation angle).

We have exploited the etalon construct for a wide variety of applications in sensing, biosensing, and drug delivery.<sup>34–37</sup> Here, to further demonstrate the utility of the etalon construct, we show that the structures can be rendered photoresponsive by exploiting the ability of AuNPs to absorb visible light and transform it into heat—the heat is capable of triggering pNIPAm-based microgel collapse, which results in a change in the etalon's optical properties. Specifically, the devices investigated here were fabricated by modifying glass coverslips with (3-aminopropyl)-trimethoxysilane (APTMS) or Au-coated glass coverslips with cysteamine—the amine termini on both substrates can be used to absorb AuNPs. Then, microgel-based etalons were fabricated on top of the AuNP layers and the optical response of the etalons to green light ( $\sim 515$  nm) supplied by a light-emitting diode (LED) investigated. We found that at all temperatures investigated below  $32$  °C the magnitude of the device's response to light irradiation increased. However, at temperatures above  $32$  °C, the microgels in the etalons were collapsed, and the etalon response to light exposure was diminished significantly. We attributed this to the fact that microgels were already collapsed at the elevated temperatures, and therefore heat supplied from the AuNPs could not cause the microgels to collapse further. Additionally, we found that the etalon response could be enhanced by adding more AuNP layers to the glass substrate prior to etalon fabrication. Since there is such a diversity of AuNP sizes, shapes, and configurations (e.g., core–shell

AuNPs) the devices could be made responsive to many different wavelengths, even wavelengths in the near-infrared range of the electromagnetic spectrum.<sup>38–41</sup> These wavelengths can penetrate relatively deeply into skin, which will allow these devices to deliver small-molecule therapeutics in a light-triggered fashion.

## EXPERIMENTAL SECTION

**Materials.** *N*-Isopropylacrylamide was purchased from TCI (Portland, Oregon) and purified by recrystallization from hexanes (ACS reagent grade, EMD, Gibbstown, NJ) prior to use. *N,N'*-Methylenebis(acrylamide) (BIS) (99%), ammonium persulfate (APS) (98.5%), DMSO, and cysteamine ( $\approx 95\%$ ) were obtained from Sigma–Aldrich (Oakville, ON) and were used as received. (3-Aminopropyl)-trimethoxysilane (APTMS) was purchased from United Chemical Technologies Inc. (Bristol, PA) and was kept in a desiccator for storage. Poly(diallyldimethylammonium chloride) (pDADMAC) was purchased from Sigma–Aldrich (St. Louis, USA). Citrate-capped gold nanoparticles (AuNPs) with 15 nm diameter were purchased from nanoComposix (San Diego, CA). Sodium chloride was obtained from Fisher Scientific (Ottawa, ON). All deionized (DI) water was filtered to have a resistivity of 18.2 M $\Omega$ ·cm and was obtained from a Milli-Q Plus system from Millipore (Billerica, MA). Chromium (Cr) and gold (Au) were deposited using a model THEUPG thermal evaporation system from Torr International Inc. (New Windsor, NY). Annealing of Cr/Au layers was done in a Thermolyne muffle furnace from Thermo Fisher Scientific (Ottawa, Ontario). Anhydrous ethanol was obtained from Commercial Alcohols (Brampton, Ontario). Fisher's finest prewashed glass coverslips were  $25 \times 25$  mm and obtained from Fisher Scientific (Ottawa, Ontario). Cr (99.999%) was obtained from ESPI (Ashland, OR), while Au (99.99%) was obtained from MRCs Canada (Edmonton, AB). The LED used was obtained from LEDynamics Inc. (part number A008-EGRN0-Q4, VT, USA), capable of supplying a luminous flux of 540 lm (at 700 mA) with a maximum intensity centered at  $\sim 515$  nm.

**Procedures.** *Poly(N-isopropylacrylamide-co-acrylic acid) Microgel Synthesis.* Microgels composed of poly(*N*-isopropylacrylamide-co-acrylic acid) (pNIPAm-co-AAc) were synthesized via temperature-ramp, surfactant-free, free radical precipitation polymerization as described previously.<sup>33</sup> The monomer mixture was comprised of 85% *N*-isopropylacrylamide (NIPAm), 10% acrylic acid (AAc), and 5% *N,N'*-methylenebis(acrylamide) (BIS) as the cross-linker. The monomer, NIPAm (17.0 mmol), and BIS (1.0 mmol) were dissolved in deionized water (100 mL) with stirring in a beaker. The mixture was filtered through a 0.2  $\mu$ m filter affixed to a 20 mL syringe into a 200 mL three-neck round-bottom flask. The beaker was rinsed with 25 mL of deionized water and then filtered into the NIPAm/BIS solution. The flask was then equipped with a temperature probe, a condenser, and a N<sub>2</sub> gas inlet (via a needle). The solution was bubbled with N<sub>2</sub> gas for  $\sim 1.5$  h, while stirring at a rate of 450 rpm, allowing the temperature to reach 45 °C. AAc (2.0 mmol) was then added to the heated mixture with a micropipette in one aliquot. A 0.078 M aqueous solution of APS (5 mL) was delivered to the reaction flask with a transfer pipet to initiate the reaction. Immediately following initiation, a temperature ramp of 45–65 °C was applied to the solution at a rate of 30 °C/h. The reaction was allowed to proceed overnight at 65 °C. After polymerization, the reaction mixture was allowed to cool to room temperature and filtered through glass wool to remove any large aggregates. The coagulum was rinsed with deionized water and filtered. Aliquots of these microgels (14 mL) were centrifuged at a speed of  $\sim 8500$  relative centrifugal force (rcf) at 23 °C for about 45 min to produce a pellet at the bottom of the centrifuge tube. The supernatant was removed from the pellet of microgels, which was then resuspended to the original volume (14 mL) using deionized water. This process was continued for a total of six times to remove any unreacted monomer and/or linear polymer from the microgel solution. Concentrated microgels were stored in the centrifuge tube for future use.

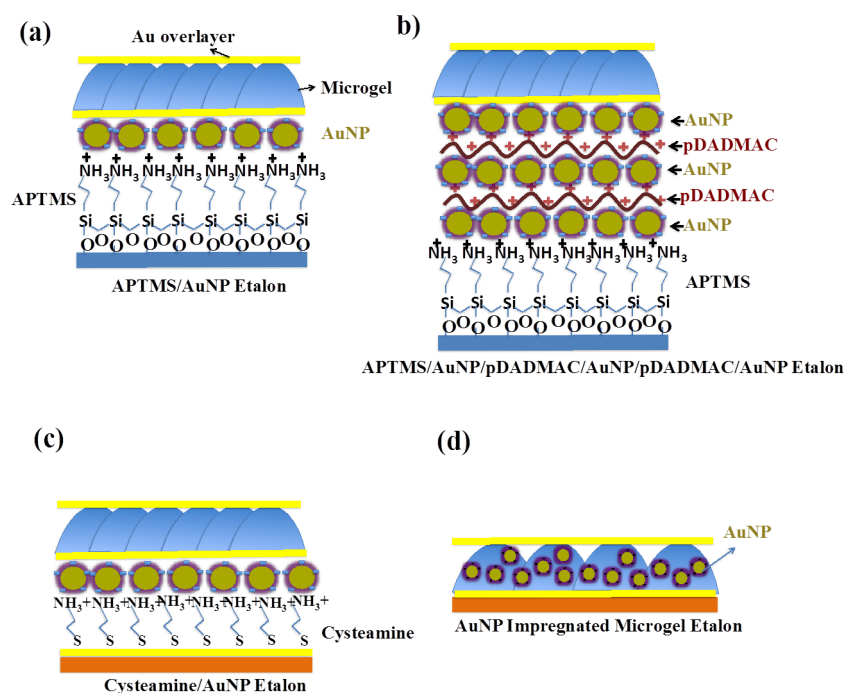


**Figure 2.** Schematic of AuNP-modified etalons. (a) APTMS/AuNPs etalons were fabricated by modifying glass coverslips with APTMS followed by deposition of a AuNP layer. Then, Cr/Au was deposited, followed by microgels, and another layer of Cr/Au. (b) APTMS/AuNPs/pDADMAC/AuNPs/pDADMAC/AuNPs etalons were generated by depositing AuNPs on an APTMS-modified glass substrate, followed by deposition of a pDADMAC layer. This layer was then exposed to the AuNP solution and then exposed again to pDADMAC—this was repeated to yield three AuNP layers, onto which a Cr/Au layer was deposited, followed by microgels, and another layer of Cr/Au. (c) Cysteamine/AuNP etalons were generated by modifying Au-coated glass substrates with cysteamine, followed by deposition of AuNPs. This substrate was then used to deposit a Cr/Au layer, followed by microgels, and another layer of Cr/Au layer. (d) AuNP impregnated etalons were generated by depositing a Cr/Au layer on a glass coverslip, followed by the addition of microgels. The microgel-coated substrate was then exposed to the AuNP solution and another layer of Cr/Au deposited.

**Substrate Functionalization and Device Fabrication.** Glass coverslips were functionalized with APTMS to allow AuNPs to adsorb to the substrates. This was done by washing glass substrates with DI water followed by rinsing with absolute ethanol. The substrates were then immersed in freshly prepared Piranha solution (4:1  $\text{H}_2\text{SO}_4/\text{H}_2\text{O}_2$ ) for 30 min, to remove any organics from the substrate surface (Caution! Piranha solutions react violently in the presence of many organic compounds and should be handled with extreme caution). The substrates were again rinsed copiously with DI water and 95% ethanol, dried with  $\text{N}_2$ , and then immersed in a solution composed of 1% APTMS (in absolute ethanol) for 2 h. After this time, the substrates were removed from the APTMS solution and once again rinsed copiously with 95% ethanol. These substrates were dipped into a solution of AuNPs (15 nm diameter, 0.055 mg/mL aqueous solution) for 30 min, then washed copiously with DI water, dried with  $\text{N}_2$  gas, and used or stored. These substrates were then used to deposit microgel-based etalons. Specifically, a 2 nm layer of Cr followed by 15 nm of Au was deposited using a thermal evaporator. Then, using a previously reported painting technique,<sup>42</sup> a monolithic monolayer of microgels was painted on the deposited Au layer, followed by the deposition of another 2 nm Cr and 15 nm Au layer on the microgels.<sup>42</sup> A schematic of the structure is shown in Figure 2a. The completed devices were soaked overnight in DI water held at 30 °C overnight before they were used for further experiments.

Slides with multiple AuNP layers were also generated using a well-established layer-by-layer approach.<sup>43–46</sup> To accomplish this, AuNP-modified substrates were exposed to a pDADMAC solution for 30 min followed by copious rinsing with DI water and dried with  $\text{N}_2$  gas. The electrostatic interaction between pDADMAC and citrate-capped AuNPs allowed the layer to be formed. The substrates were then exposed to the AuNP solution again, followed by rinsing, drying, and exposure to the pDADMAC solution. This process was repeated until three layers of AuNPs were achieved (APTMS/AuNPs/pDADMAC/

AuNPs/pDADMAC/AuNPs). Once this multilayer film was achieved, the etalon construct was deposited on top, as detailed above. This can be seen schematically in Figure 2b.

For other investigations, clean glass coverslips were directly coated with 2 nm of Cr followed by 15 nm of Au via thermal evaporation followed by annealing at 250 °C for 3 h. The Cr/Au-coated substrates were immersed into a solution of cysteamine (1% aqueous solution; 2 h), washed copiously with DI water, and dried with  $\text{N}_2$  gas. Cysteamine was adsorbed onto the slides by strong interaction of thiol and Au, whereas cysteamine's  $\text{NH}_2$  was free to react with other groups.<sup>47</sup> The substrates were then used to adsorb AuNPs by dipping them in a solution of AuNPs. The pH of the AuNP solution (pH = 5.9) allowed the cysteamine's amine to be protonated and form a strong bond with AuNPs. The resulting substrates were washed copiously with DI water, dried with  $\text{N}_2$ , and used to deposit an etalon on top using the same procedure described above. This is shown schematically in Figure 2c.

Finally, etalons were fabricated directly on Au-coated glass substrates, and the AuNPs impregnated into the microgel layer. To accomplish this, 2 nm of Cr followed by 15 nm of Au was deposited onto a clean glass coverslip, followed by deposition of microgels using the painting protocol, then exposed the AuNP solution for 30 min to allow the AuNPs to adsorb into/onto the microgels.<sup>48,49</sup> The substrates were washed copiously with DI water, dried, and coated with 2 nm of Cr followed by 15 nm of Au. The structure of this device can be seen in Figure 2d.

**Reflectance Spectroscopy.** Reflectance spectra were collected using a USB2000+ spectrophotometer, an HL-2000-FHSA tungsten light source, and an R400-7-VIS-NIR optical fiber reflectance probe all from Ocean Optics (Dunedin, FL). The spectra were recorded using Ocean Optics Spectra Suite Spectroscopy Software over a wavelength range of 350–1025 nm. The sample was fixed in a Petri dish filled with aqueous solution of pH = 3.0 (prepared by adding 1 M HCl solution

to DI water) and was positioned over a LED source of green light ( $\sim 515$  nm)—the typical distance between the LED and the etalon was 0.5 cm. The water temperature was monitored with a digital thermometer. The optical fiber reflectance probe was positioned over the sample with a clamp so that the location and height of the light source was fixed and controlled to get the best reflectance spectrum (i.e., well-defined reflectance peaks) as shown in Figure 3. A

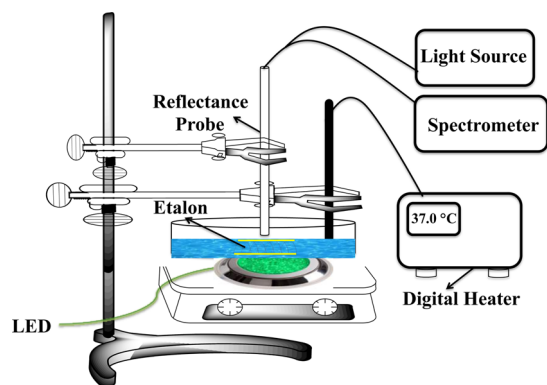


Figure 3. Simplified schematic diagram of the experimental setup.

heating probe and a test tube filled with crushed ice were dipped into the Petri dish, which allowed the temperature to be controlled to 0.5 °C. Spectra were monitored and recorded at specific temperatures. It is important to note that spectra were collected once the position of the spectral peaks ceased shifting and turned the LED off.

## RESULTS AND DISCUSSION

First, we investigated the response of APTMS/AuNPs etalons to LED light exposure; the AuNPs used here had a  $\lambda_{\text{max}}$  of  $\sim 517$  nm. The UV–vis spectrum for the AuNPs used here in aqueous solution can be seen in Figure S1 of the Supporting Information (SI). As can be seen in Figure 4a and 4b, the

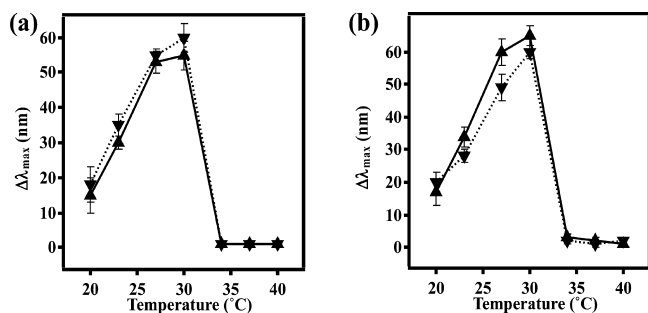


Figure 4. Change in position of a single reflectance peak ( $\Delta\lambda_{\text{max}}$ ) for (a) APTMS/AuNPs etalon and (b) cysteamine/AuNPs etalon while the LED was turned on. The LED light source was turned on for  $\sim 30$  min for each time to record the shift in reflectance spectra. Here, symbol ( $\blacktriangle$ ) indicates the temperature increase cycle, while symbol ( $\blacktriangledown$ ) denotes the temperature decrease cycle. Each data point represents the average of at least three independent measurements on the same device, and the error bars are the standard deviation for those values.

APTMS/AuNPs and cysteamine/AuNPs etalons exhibited a large spectral response (spectral blue shift) upon exposure to the green LED ( $\sim 30$  min, which is the time required to yield a stable reflectance peak position) at temperatures below 32 °C. We point out here that the time for the devices to respond was relatively fast, although 30 min was often required to ensure the optical properties of the devices were completely stable. For all

devices, we measured the reflectance peak near 700 nm—since the devices were made from the same microgels, this ensured that the same order peak was being monitored from sample to sample. It should also be noted that the magnitude of the shift increased with increasing temperature up to 32 °C. We attribute the light-triggered optical response to the AuNPs absorbing the green LED light followed by a release of heat into the local environment near the microgels. We hypothesize that the heat released from the AuNPs causes the pNIPAm-based microgels to collapse, resulting in the observed spectral shift. As the temperature of the environment approaches pNIPAm's LCST, the devices become more sensitive to light exposure due to the fact that the AuNP heating could more easily increase the local temperature to above pNIPAm's LCST; this results in large responses relative to devices held at a temperature far away from pNIPAm's LCST. This hypothesis is supported by the lack of etalon response to light exposure as the environmental temperature exceeds the LCST; this is because the microgels are already fully collapsed, and the heat generated by the AuNPs has no effect on microgel diameter. Importantly, we found that the optical properties of the etalons were completely reversible over a number of cycles without an obvious loss in function, as can be seen in Figure 5.

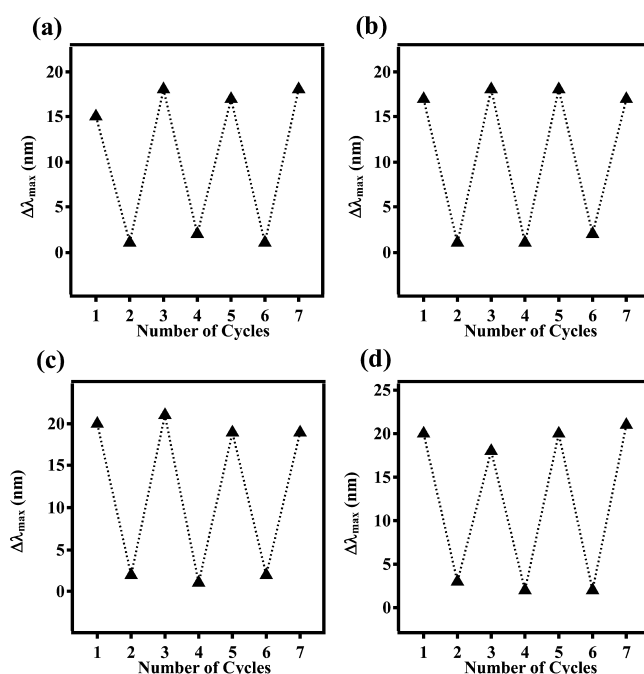
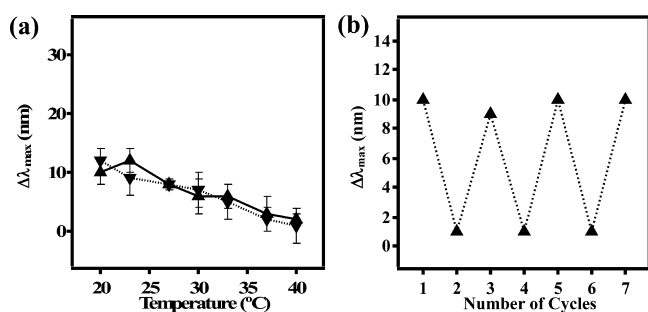


Figure 5. Shift in reflectance peak ( $\lambda_{\text{max}}$ ) of (a) APTMS/AuNPs etalon; (b) cysteamine/AuNPs etalon; (c) APTMS/AuNPs/pDADMAC/AuNPs/pDADMAC/AuNPs etalon, and (d) AuNPs impregnated etalon devices. Here, each odd number indicates that the LED was on, and the even number indicates that the LED was off. The environmental temperature was 20 °C for these experiments. The LED light source was turned on for  $\sim 30$  min for each time to record the shift in reflectance spectra.

To confirm that the observed response was a result of the AuNPs, we fabricated an etalon by painting a monolithic microgel layer on top of a Cr/Au-coated glass coverslip and subsequently adding another Au layer on top. It should be noted here that this device does not have a AuNP layer present. We found that exposure of this device to the LED light source had minimal impact on the optical properties of the etalon, as

shown in Figure 6. For these experiments, the light was turned on for 30 min, and while there is a response, it is small relative



**Figure 6.** (a) Position of a single reflectance peak ( $\lambda_{\max}$ ) for etalons without AuNPs. Here, symbol ( $\blacktriangle$ ) indicates the temperature increase cycle, while symbol ( $\blacktriangledown$ ) denotes the temperature decrease cycle. Each data point represents the average of at least three independent measurements on the same device, and the error bars are the standard deviation for those values. The LED light was turned on for 30 min or until the device ceased the movement in reflectance spectra. (b) The cycle of LED on and off with the same device at 20 °C. Here, each odd number indicates that the LED was on, and an even number indicates that the LED was off.

to the response of the device composed of AuNPs. This may be a result of the Au layer of the etalon absorbing some of the light energy, resulting in some local heating. Similar to the above devices, these etalons did not respond to light at temperatures higher than 32 °C.

Since we attributed the response of the etalon to the heat generated from the AuNPs absorbing the green LED light, followed by heat dissipation and microgel collapse, we investigated whether more AuNP layers in a device could yield an enhanced response. Figure 7 shows the spectral

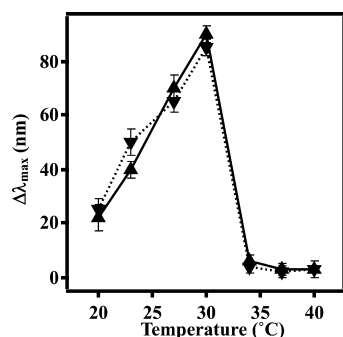


**Figure 7.** Position of a single reflectance peak ( $\lambda_{\max}$ ) for the APTMS/AuNPs/pDADMAC/AuNPs/pDADMAC/AuNPs etalon. Here, symbol ( $\blacktriangle$ ) indicates the temperature increase cycle, while symbol ( $\blacktriangledown$ ) denotes the temperature decrease cycle. Each data point represents the average of at least three independent measurements on the same device, and the error bars are the standard deviation for those values. The LED light was turned on for 30 min or until the device ceased the movement in reflectance spectra.

response of devices composed of three AuNP layers upon exposure to the LED source for 30 min. As can be seen, the shift in the spectral peak of the reflectance spectrum is enhanced in magnitude compared to the devices composed of a single layer. Also, the sensitivity to LED exposure increased linearly below 32 °C, and above that temperature no response was observed. This device can also be cycled between LEDs on

and off at fixed temperature (Figure 5c) that proves that they can be actuated repeatedly.

Finally, we wanted to investigate the light-induced response of etalons with AuNPs impregnated directly into the microgel layer. Figure 8 shows that the peaks in the reflectance spectrum

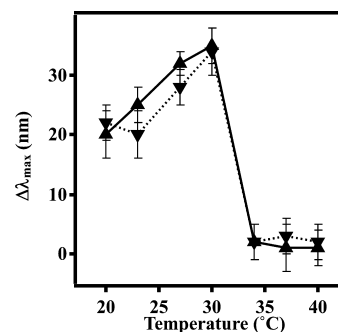


**Figure 8.** Shift in the position of a single reflectance peak ( $\lambda_{\max}$ ) of a AuNP impregnated device at different temperatures. Here, symbol ( $\blacktriangle$ ) indicates LED on cycle, while symbol ( $\blacktriangledown$ ) denotes LED off cycle. Here each data point represents the average of at least three independent measurements on the same device, and the error bars are the standard deviation for those values. The LED light was turned on until the shift was ceased (usually  $\approx$ 30 min).

shifted significantly upon exposure to the LED for 30 min. We attribute this to the photothermal effect of impregnated AuNPs, which absorb radiation and release heat resulting in an increase in the temperature of the solution in the microgels. As a result, the microgels collapse and reduce the distance between the etalon's Cr/Au layers resulting in a shift in the reflectance spectrum. These devices can be actuated repeatedly by turning the LED light on and off as can be seen from Figure 5d.

## CONCLUSION

We were able to show that pNIPAm microgel-based etalons can be fabricated and made sensitive to light exposure by doping the devices with AuNPs—AuNPs are well-known to absorb light of certain wavelengths and concomitantly release heat into the local environment. We found that the sensitivity of the devices to LED exposure increased linearly with temperature below 32 °C. Above this temperature, the devices were not responsive. We attribute this to the fact that the microgels are already collapsed above 32 °C, so further heating by the AuNPs had no effect on the optical properties. We also found that multilayers of AuNPs can be added to the substrate to enhance the sensitivity of the devices to light exposure. Finally, we showed that the response of the devices could be cycled many times without significant hysteresis. These devices could be made such that they respond to wavelengths capable of penetrating deep into skin, allowing them to be used for triggered/controlled drug delivery.

## ASSOCIATED CONTENT

### Supporting Information

The Supporting Information is available free of charge on the ACS Publications website at DOI: 10.1021/acsami.5b08532.

Additional Figures S1 and S2 (PDF)

## AUTHOR INFORMATION

### Corresponding Author

\*E-mail: michael.serpe@ualberta.ca.

## Present Address

<sup>†</sup>Schmid College of Science and Technology, Chapman University, Orange, CA 92866.

## Notes

The authors declare no competing financial interest.

## ACKNOWLEDGMENTS

MJS acknowledges funding from the University of Alberta (the Department of Chemistry and the Faculty of Science), the Natural Sciences and Engineering Research Council of Canada (NSERC), the Canada Foundation for Innovation (CFI), the Alberta Advanced Education & Technology Small Equipment Grants Program (AET/SEGP), and Grand Challenges Canada and IC-IMPACTS.

## REFERENCES

- (1) Katz, E.; Willner, I. Integrated Nanoparticle–Biomolecule Hybrid Systems: Synthesis, Properties, and Applications. *Angew. Chem., Int. Ed.* **2004**, *43* (45), 6042–6108.
- (2) Niemeyer, C. M. Nanoparticles, Proteins, and Nucleic Acids: Biotechnology Meets Materials Science. *Angew. Chem., Int. Ed.* **2001**, *40* (22), 4128–4158.
- (3) Buck, M. R.; Schaak, R. E. Emerging Strategies for the Total Synthesis of Inorganic Nanostructures. *Angew. Chem., Int. Ed.* **2013**, *52* (24), 6154–6178.
- (4) Rosi, N. L.; Mirkin, C. A. Nanostructures in Biagnostics. *Chem. Rev.* **2005**, *105* (4), 1547–1562.
- (5) Zhang, L.; Roling, L. T.; Wang, X.; Vara, M.; Chi, M.; Liu, J.; Choi, S.-I.; Park, J.; Herron, J. A.; Xie, Z.; Mavrikakis, M.; Xia, Y. Platinum-based Nanocages with Subnanometer-thick Walls and Well-defined, Controllable Facets. *Science* **2015**, *349* (6246), 412–416.
- (6) Roper, D. K.; Ahn, W.; Hoepfner, M. Microscale Heat Transfer Transduced by Surface Plasmon Resonant Gold Nanoparticles. *J. Phys. Chem. C* **2007**, *111* (9), 3636–3641.
- (7) Hu, M.; Hartland, G. V. Heat Dissipation for Au Particles in Aqueous Solution: Relaxation Time versus Size. *J. Phys. Chem. B* **2002**, *106* (28), 7029–7033.
- (8) Jain, P. K.; Lee, K. S.; El-Sayed, I. H.; El-Sayed, M. A. Calculated Absorption and Scattering Properties of Gold Nanoparticles of Different Size, Shape, and Composition: Applications in Biological Imaging and Biomedicine. *J. Phys. Chem. B* **2006**, *110* (14), 7238–7248.
- (9) Kim, D.; Park, S.; Lee, J. H.; Jeong, Y. Y.; Jon, S. Antibiofouling Polymer-Coated Gold Nanoparticles as a Contrast Agent for in Vivo X-ray Computed Tomography Imaging. *J. Am. Chem. Soc.* **2007**, *129* (24), 7661–7665.
- (10) Saha, K.; Agasti, S. S.; Kim, C.; Li, X.; Rotello, V. M. Gold Nanoparticles in Chemical and Biological Sensing. *Chem. Rev.* **2012**, *112* (5), 2739–2779.
- (11) Brown, A. C.; Stabenfeldt, S. E.; Ahn, B.; Hannan, R. T.; Dhada, K. S.; Herman, E. S.; Stefanelli, V.; Guzzetta, N.; Alexeev, A.; Lam, W. A.; Lyon, L. A.; Barker, T. H. Ultrasoft Microgels Displaying Emergent Platelet-like Behaviours. *Nat. Mater.* **2014**, *13* (12), 1108–1114.
- (12) Smith, M. H.; Lyon, L. A. Multifunctional Nanogels for siRNA Delivery. *Acc. Chem. Res.* **2012**, *45* (7), 985–993.
- (13) Hoare, T.; Pelton, R. Highly pH and Temperature Responsive Microgels Functionalized with Vinylacetic Acid. *Macromolecules* **2004**, *37* (7), 2544–2550.
- (14) Islam, M. R.; Serpe, M. J. Polymer-Based Devices for the Label-Free Detection of DNA in Solution: Low DNA Concentrations Yield Large Signals. *Anal. Bioanal. Chem.* **2014**, *406* (19), 4777–4783.
- (15) Wong, J. E.; Gaharwar, A. K.; Mueller-Schulte, D.; Bahadur, D.; Richtering, W. Dual-stimuli Responsive PNIPAM Microgel Achieved via Layer-by-layer Assembly: Magnetic and Thermo-responsive. *J. Colloid Interface Sci.* **2008**, *324* (1–2), 47–54.
- (16) Pich, A.; Richtering, W. Microgels by Precipitation Polymerization: Synthesis, Characterization, and Functionalization. *Adv. Polym. Sci.* **2010**, *234* (Chemical Design of Responsive Microgels), 1–37.
- (17) Hoare, T.; Pelton, R. Engineering Glucose Swelling Responses in Poly(N-isopropylacrylamide)-Based Microgels. *Macromolecules* **2007**, *40* (3), 670–678.
- (18) Jones, C. D.; Serpe, M. J.; Schroeder, L.; Lyon, L. A. Microlens Formation in Microgel/Gold Colloid Composite Materials via Photothermal Patterning. *J. Am. Chem. Soc.* **2003**, *125* (18), 5292–5293.
- (19) Wu, C.; Wang, X. H. Globule-to-Coil Transition of a Single Homopolymer Chain in Solution. *Phys. Rev. Lett.* **1998**, *80* (18), 4092.
- (20) Scherzinger, C.; Schwarz, A.; Bardow, A.; Leonhard, K.; Richtering, W. Cononsolvency of poly-N-isopropyl acrylamide (PNIPAM): Microgels versus linear chains and macrogels. *Curr. Opin. Colloid Interface Sci.* **2014**, *19* (2), 84–94.
- (21) Hu, X.; Tong, Z.; Lyon, L. A. Multicompartment Core/Shell Microgels. *J. Am. Chem. Soc.* **2010**, *132* (33), 11470–11472.
- (22) Nayak, S.; Lyon, L. A. Soft Nanotechnology with Soft Nanoparticles. *Angew. Chem., Int. Ed.* **2005**, *44* (47), 7686–7708.
- (23) Suzuki, A.; Tanaka, T. Phase Transition in Polymer Gels Induced by Visible Light. *Nature* **1990**, *346* (6282), 345–347.
- (24) Serphen, S. R.; Mensing, G. A.; Ng, M.; Halas, N. J.; Beebe, D. J.; West, J. L. Independent Optical Control of Microfluidic Valves Formed from Optomechanically Responsive Nanocomposite Hydrogels. *Adv. Mater.* **2005**, *17* (11), 1366–1368.
- (25) Wang, E.; Desai, M. S.; Lee, S.-W. Light-Controlled Graphene-Elastin Composite Hydrogel Actuators. *Nano Lett.* **2013**, *13* (6), 2826–2830.
- (26) Kim, D.; Lee, H. S.; Yoon, J. Remote Control of Volume Phase Transition of Hydrogels Containing Graphene Oxide by Visible Light Irradiation. *RSC Adv.* **2014**, *4* (48), 25379–25383.
- (27) Hauser, A. W.; Evans, A. A.; Na, J.-H.; Hayward, R. C. Photothermally Reprogrammable Buckling of Nanocomposite Gel Sheets. *Angew. Chem., Int. Ed.* **2015**, *54* (18), 5434–5437.
- (28) Hoare, T.; Pelton, R. Functional Group Distributions in Carboxylic Acid-Containing Poly(N-isopropylacrylamide) Microgels. *Langmuir* **2004**, *20* (6), 2123–2133.
- (29) Scherzinger, C.; Lindner, P.; Keerl, M.; Richtering, W. Cononsolvency of Poly(N,N-diethylacrylamide) (PDEAAM) and Poly(N-isopropylacrylamide) (PNIPAM) Based Microgels in Water/Methanol Mixtures: Copolymer vs. Core-Shell Microgel. *Macromolecules (Washington, DC, U. S.)* **2010**, *43* (16), 6829–6833.
- (30) Sigolaeva, L. V.; Gladys, S. Y.; Gelissen, A. P. H.; Mergel, O.; Pergushov, D. V.; Kurochkin, I. N.; Plamper, F. A.; Richtering, W. Dual-Stimuli-Sensitive Microgels as a Tool for Stimulated Sponglike Adsorption of Biomaterials for Biosensor Applications. *Biomacromolecules* **2014**, *15* (10), 3735–3745.
- (31) Islam, M. R.; Serpe, M. J. Penetration of Polyelectrolytes into Charged Poly(N-isopropylacrylamide) Microgel Layers Confined between Two Surfaces. *Macromolecules (Washington, DC, U. S.)* **2013**, *46* (4), 1599–1606.
- (32) Sorrell, C. D.; Carter, M. C. D.; Serpe, M. J. Color tunable poly(N-isopropylacrylamide)-co-acrylic acid microgel-Au hybrid assemblies. *Adv. Funct. Mater.* **2011**, *21* (3), 425–433.
- (33) Sorrell, C. D.; Serpe, M. J. Reflection Order Selectivity of Color-Tunable Poly(N-isopropylacrylamide) Microgel Based Etalons. *Adv. Mater. (Weinheim, Ger.)* **2011**, *23* (35), 4088–4092.
- (34) Islam, M. R.; Serpe, M. J. Label-free detection of low protein concentration in solution using a novel colorimetric assay. *Biosens. Bioelectron.* **2013**, *49*, 133–138.
- (35) Islam, M. R.; Serpe, M. J. A novel label-free colorimetric assay for DNA concentration in solution. *Anal. Chim. Acta* **2014**, *843*, 83–88.
- (36) Gao, Y.; Ahiabu, A.; Serpe, M. J. Controlled Drug Release from the Aggregation-Disaggregation Behavior of pH-Responsive Microgels. *ACS Appl. Mater. Interfaces* **2014**, *6* (16), 13749–13756.

- (37) Huang, H.; Serpe, M. J. Poly(N-isopropylacrylamide) Microgel-Based Etalons for Determining the Concentration of Ethanol in Gasoline. *J. Appl. Polym. Sci.* **2015**, *132* (24), 42106 (1–6).
- (38) Mukherjee, S.; Zhou, L.; Goodman, A. M.; Large, N.; Ayala-Orozco, C.; Zhang, Y.; Nordlander, P.; Halas, N. J. Hot-Electron-Induced Dissociation of H<sub>2</sub> on Gold Nanoparticles Supported on SiO<sub>2</sub>. *J. Am. Chem. Soc.* **2014**, *136* (1), 64–67.
- (39) Personick, M. L.; Langille, M. R.; Zhang, J.; Mirkin, C. A. Shape Control of Gold Nanoparticles by Silver Underpotential Deposition. *Nano Lett.* **2011**, *11* (8), 3394–3398.
- (40) Xia, X.; Zeng, J.; Zhang, Q.; Moran, C. H.; Xia, Y. Recent Developments in Shape-Controlled Synthesis of Silver Nanocrystals. *J. Phys. Chem. C* **2012**, *116* (41), 21647–21656.
- (41) Puentes, V. F.; Krishnan, K. M.; Alivisatos, A. P. Colloidal Nanocrystal Shape and Size Control: The Case of Cobalt. *Science* **2001**, *291* (5511), 2115–2117.
- (42) Sorrell, C. D.; Carter, M. C. D.; Serpe, M. J. A "Paint-On" Protocol for the Facile Assembly of Uniform Microgel Coatings for Color Tunable Etalon Fabrication. *ACS Appl. Mater. Interfaces* **2011**, *3* (4), 1140–1147.
- (43) Decher, G.; Hong, J.-D. Buildup of Ultrathin Multilayer Films by a Self-Assembly Process. I. Consecutive Adsorption of Anionic and Cationic Bipolar Amphiphiles on Charged Surfaces. *Makromol. Chem., Macromol. Symp.* **1991**, *46* (1), 321–327.
- (44) Decher, G. Fuzzy Nanoassemblies: Toward Layered Polymeric Multicomposites. *Science* **1997**, *277* (5330), 1232–1237.
- (45) Serpe, M. J.; Jones, C. D.; Lyon, L. A. Layer-by-Layer Deposition of Thermoresponsive Microgel Thin Films. *Langmuir* **2003**, *19* (21), 8759–8764.
- (46) Decher, G.; Hong, J. D.; Schmitt, J. Buildup of Ultrathin Multilayer Films by a Self-Assembly Process: III. Consecutively Alternating Adsorption of Anionic and Cationic Polyelectrolytes on Charged Surfaces. *Thin Solid Films* **1992**, *210–211*, 831–835.
- (47) Riauba, L.; Niaura, G.; Eicher-Lorka, O.; Butkus, E. A Study of Cysteamine Ionization in Solution by Raman Spectroscopy and Theoretical Modeling. *J. Phys. Chem. A* **2006**, *110* (50), 13394–13404.
- (48) Kozlovskaya, V.; Kharlampieva, E.; Khanal, B. P.; Manna, P.; Zubarev, E. R.; Tsukruk, V. V. Ultrathin Layer-by-Layer Hydrogels with Incorporated Gold Nanorods as pH-Sensitive Optical Materials. *Chem. Mater.* **2008**, *20* (24), 7474–7485.
- (49) Park, C.; South, A.; Hu, X.; Verdes, C.; Kim, J.-D.; Lyon, L. A. Gold Nanoparticles Reinforce Self-Healing Microgel Multilayers. *Colloid Polym. Sci.* **2011**, *289* (5–6), 583–590.

# Supporting Information

## Photothermally Induced Optical Property Changes of Poly (*N*-isopropylacrylamide) Microgel-Based Etalons

Molla R. Islam,<sup>§</sup> Jessica Irvine, and Michael J. Serpe\*

Department of Chemistry, University of Alberta, Edmonton, AB, T6G 2G2

\*Corresponding Author: Michael J. Serpe (michael.serpe@ualberta.ca)

§ Current Address: Schmid College of Science and Technology, Chapman University, Orange, CA 92866

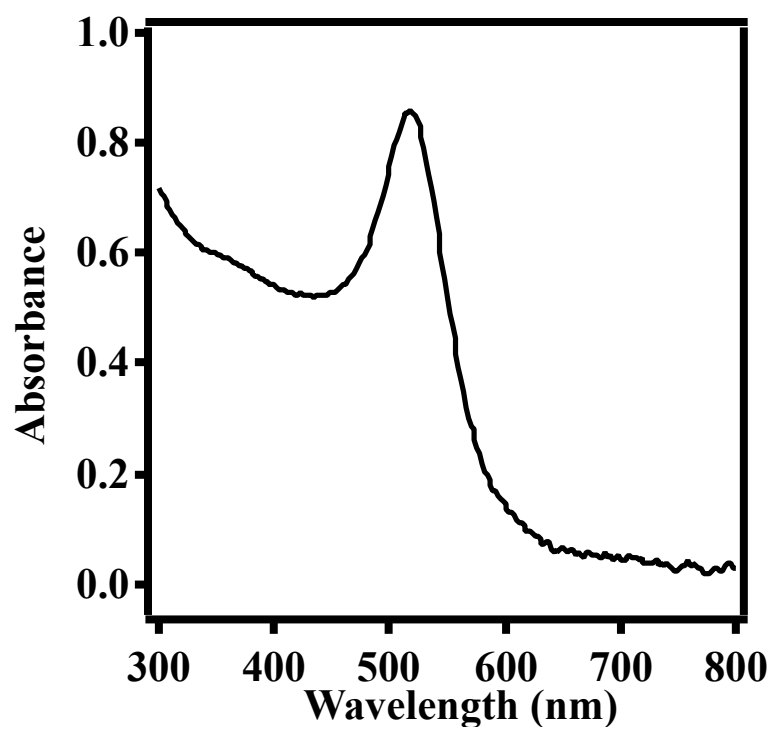


Fig. S1. UV-Vis spectrum of the AuNPs used in this study in solution.

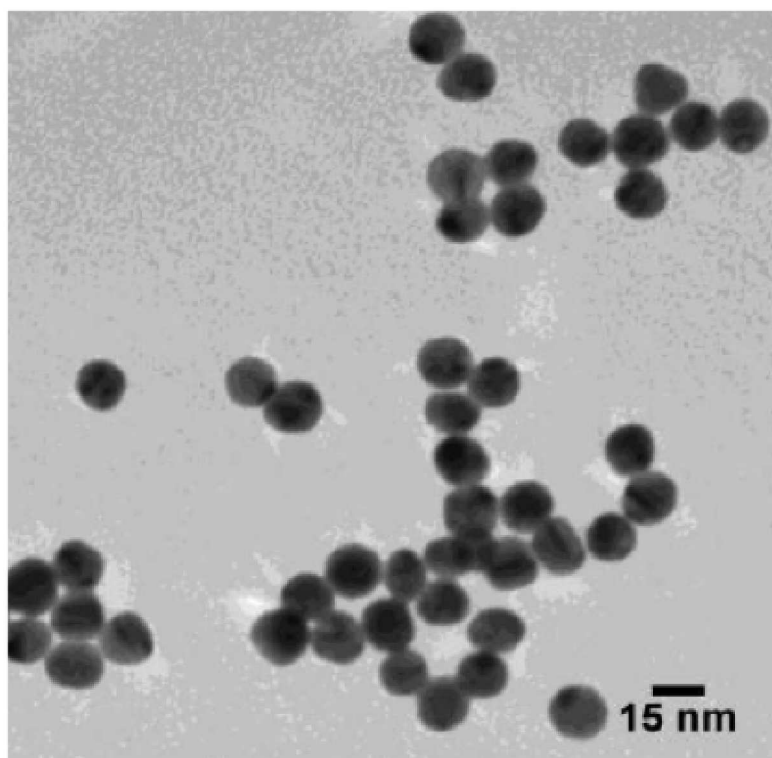


Fig. S2. Transmission electron microscope image of the AuNPs used in this study.